https://doi.org/10.5194/egusphere-2026-3760
Preprint. Discussion started: 7 July 2026

Contrasting Roles of Microbial Heterogeneity and Sediment Heterogeneity in Controlling Hyporheic Nitrogen Removal

Yang Xian[1], Zhang Wen[1,2*], and Stefan Krause[3]

[1] Hubei Key Laboratory of Yangtze Catchment Environmental Aquatic Science, School of Environmental Studies, China University of Geosciences, Wuhan, 430078, Hubei, P. R. China

[2] State Key Laboratory of Biogeology and Environmental Geology, China University of Geosciences, Wuhan, 430078, Hubei, P. R. China

[3] School of Geography, Earth and Environmental Sciences, University of Birmingham, UK

[*]Corresponding author: Zhang Wen (wenz@cug.edu.cn)

https://doi.org/10.5194/egusphere-2026-3760
Preprint. Discussion started: 7 July 2026

Abstract

Bacteria in streambed sediments reduce nitrogen pollution by performing chemical reactions that can transform pollutants. However, how differences in sediment types (like sandy vs. clay-rich layers) or the distribution of these bacteria affect the nitrogen removal in streambed sediments remains unclear. To explore this, we built numerical models to mimic real streambed conditions and explore how small-scale variations in sediment and microbial communities influence nitrogen removal. Our results show that the spatial changes in physical and chemical properties of sediments (e.g., permeability and organic matter content) have little impact on nitrogen removal. Instead, variations in the distribution of nitrogen-processing microbes are far more critical. This is because bacteria and the sticky substances they produce can slowly clog the sediment pores. This clogging limits the movement of pollution to the very top layers of sediments, making deeper sediment differences irrelevant to overall nitrogen removal. These results mean that future numerical models aiming to predict nitrogen removal should focus on mapping where these helpful microbes live, rather than overcomplicating simulations with too much detail about sediment variations. Simplifying sediment assumptions could make models more practical while still capturing the key role of microbes in cleaning streams.

https://doi.org/10.5194/egusphere-2026-3760
Preprint. Discussion started: 7 July 2026

1 Introduction

High concentrations of nitrate (NO_3^-) in stream ecosystems poses severe risks to water quality, impacting both human and ecosystem health (Grant et al.,2018; Gruber & Galloway, 2008). Hyporheic zones (HZs) within streambed sediments are increasingly recognized as essential biogeochemical hotspots for nitrate attenuation (Boano et al., 2014; Harvey & Gooseff, 2015; Krause et al., 2017, 2022). The high surface area of streambed sediments and nutrient exchange fluxes across HZs create ideal conditions for microbial communities to flourish, facilitating diverse biogeochemical reactions that markedly exceed those in the overlying water column (Chowdhury et al., 2020; Gu et al., 2007). The efficiency of nitrate removal within these streambed sediments is theoretically governed by solute residence time distributions and spatially heterogeneous mixing of solutes from different water sources (Krause et al., 2022), and biogeochemical reaction rates (Zarnetske et al., 2012; Xian et al., 2023). Metabolically relevant residence time is influenced by the hyporheic flow field, which is intrinsically linked to sediment permeability, while biogeochemical reaction rates are shaped by many factors such as NO_3^- concentration, dissolved oxygen (DO) levels, dissolved organic carbon (DOC) availability, and microbial activity (Gomez-Velez et al., 2015; Stegen et al., 2018). Denitrification, the primary biogeochemical process that converts NO_3^- to nitrogen gases (N_2, N_2O), is primarily regulated by thermodynamic conditions, being inhibited by the presence of oxygen but stimulated by bioavailable DOC (Martínez-Espinosa et al., 2021; Zarnetske et al., 2011). Denitrification based nitrate removal necessitates anoxic conditions fostered by prolonged residence times and ample DOC available to facilitate DO consumption (Sawyer, 2015).

Heterogeneous fluvial sediments, encompassing fine-grained (e.g., silt and clay) and coarse-grained (e.g., gravel and sand) facies, are prevalent in riverine systems (Cardenas, 2004;

https://doi.org/10.5194/egusphere-2026-3760
Preprint. Discussion started: 7 July 2026

Sawyer & Cardenas, 2009; Gomez-Velez et al., 2014). It is well-established that this sedimentary heterogeneity generates substantial spatial variability in both physical (e.g., permeability) and chemical (e.g., organic matter (OM) content) properties (Briggs et al., 2015; Chen et al., 2025; Pescimoro et al., 2019; Sawyer, 2015). Fine sediments exhibit organic rich sediments are often characterized by lower permeability than their coarse grain, low organic counterparts. As oxygen-rich stream water permeates the streambed sediments, the heterogeneity in physical and chemical properties promote the formation of anoxic microzones essential for denitrification (Claret et al., 1997; Knights et al., 2017; Krause et al., 2013). Oxic and anoxic waters converge at the localized interfaces within the heterogeneous sediments, fostering microsites of elevated denitrification activity (Sawyer, 2015; Xian et al., 2023; Zhang et al., 2026). Such microscale mixing enhances nitrate removal efficiency in heterogeneous sediments relative to homogeneous sediment systems. For example, Sawyer (2015) has indicated that nitrate removal rates in heterogeneous sediments may exceed those of comparable homogeneous sediments by as much as sixtyfold. Recent studies (e.g., Barnes et al., 2019; Pescimoro et al., 2019; Ping et al., 2022; Wallace et al., 2020, 2021; Chen et al., 2024) have further illustrated that mixing processes within heterogeneous sediments may significantly influence nutrient transformation zones and nitrogen removal efficacy within riparian and hyporheic zones (HZs).

Despite these advances, the mechanisms by which heterogeneous sediments affect nitrate attenuation in HZs remain not fully understood. Prior studies typically consider only permeability heterogeneity (e.g., Bardini et al., 2013) or the combined effects of permeability and OM content (e.g., Barnes et al., 2019; Pescimoro et al., 2019; Sawyer, 2015; Chen et al., 2024), assuming uniform functional biomass distribution across coarse and fine structures. However, beyond the physical and chemical heterogeneity of sediments, heterogeneous

https://doi.org/10.5194/egusphere-2026-3760
Preprint. Discussion started: 7 July 2026

hyporheic systems also host spatial variability of functional groups of microorganisms responsible for biogeochemical processes (De Falco et al., 2018). Hyporheic microbiota play multiple roles in nutrient cycling within HZs (Caruso et al., 2017; Chowdhury et al., 2020; Ping et al., 2020; Xian et al., 2022; Zhang et al., 2024; Zhang et al., 2026): First, microbial communities drive numerous biogeochemical transformations, determining the spatial distribution of reaction rates. Second, microbial biofilms that are aggregations of bacterial cells embedded in self-secreted extracellular polymeric substances occupy pore spaces on sediment surfaces, modulating permeability and thus, potentially altering local flow fields. Biofilm growth introduces complex feedback mechanisms with porous media flow and reactive transport. Hyporheic flow on one hand influences biofilm development, which in turn modifies nutrient advection rates. Through these interactions, microbial functional biomass distributions become heterogeneously organized in both space and time.

This study aims to elucidate the effects of microbial heterogeneity and heterogeneity in sedimentary physical properties (e.g., permeability) and chemical composition (e.g., OM content)) on nitrate removal in HZs. This will be achieved by establishing a series of numerical models coupling porous flow, nutrient transport, and biofilm growth in heterogeneous sediments, comparing results to the equivalent homogeneous counterparts. Our findings reveal that microbial heterogeneity exerts a decisive influence on enhanced nitrogen removal within hyporheic zones, while the effect of small-scale sedimentary heterogeneity appears negligible. These insights challenge the conventional view that sedimentary heterogeneity is the primary driver of enhanced nitrate removal, highlighting the critical role of microbial heterogeneity in biogeochemical processes.

https://doi.org/10.5194/egusphere-2026-3760
Preprint. Discussion started: 7 July 2026

2 Porous Media Flow, Nutrient Dynamics and Biofilm Growth Models

In this section, we develop a suite of two-dimensional (2-D) reactive transport models for describing nitrogen dynamics of HZs in heterogeneous streambed sediments. The models are established by coupling porous media flow, reactive transport of nutrients, biofilm growth and, most importantly, their feedback mechanisms. Specifically, the processes of porous media flow, heterotrophic metabolisms of carbon and nitrogen, microbial biomass growth, endogenous decay of biomass, and bioclogging are simulated for typical small-scale ripple-induced HZs in heterogeneous sediments.

2.1 Governing Equations

The porous media flow in streambed sediments is simulated with the hydraulic continuity equation and Darcy's law, given by (Caruso et al., 2017; Zhang et al., 2024):

$$\frac{\partial \theta}{\partial t} = \nabla \cdot (K \nabla h) \tag{1}$$

where θ is the porosity, t denotes time, K represents hydraulic conductivity, and h is the hydraulic head.

The reactive transport of nutrients in HZs is described with the advection-dispersion-reaction equation:

$$\frac{\partial \theta C_i}{\partial t} = \nabla \cdot \theta D \nabla C_i - \nabla \cdot qC + R_i \tag{2}$$

where C_i denotes the solute concentration of solute i, and q is the Darcy's velocity, R_i represents the source/sink term, D denotes the hydrodynamic dispersion tensor and is expressed as (Sawyer, 2015):

https://doi.org/10.5194/egusphere-2026-3760
Preprint. Discussion started: 7 July 2026

$$D_{ij} = \alpha_T |v| \delta_{ij} + (\alpha_L - \alpha_T) \frac{v_i v_j}{|v|} + \tau D_0 \delta_{ij} \quad (3)$$

where α_L and α_T are the longitudinal and traverse dispersivities, respectively; v denotes the pore velocity and equals q/θ; τ is the tortuosity and is calculated as $\theta^{1/3}$, D_0 reprensents the molecular diffusion coefficient in water.

The key reactive solutes DOC, DO, NO_3^- are considered in the stream and the hyporheic system. The nutrients can be consumed by heterotrophic microorganisms via aerobic respiration and denitrification:

Aerobic Respiration $\quad CH_2O + O_2 \rightarrow CO_2 + H_2O$

Denitrification $\quad 5CH_2O + 4NO_3^- + 4H^+ \rightarrow 7H_2O + 5CO_2 + 2N_2$

These microbially mediated biogeochemical reactions can be modeled by multiple-Monod kinetic equation (e.g., Gu et al., 2007; Molz et al., 1986). In sediments, the particulate organic carbon (POC) can release DOC by kinetic dissolution, which can be described by first-order kinetics (Gu et al., 2007; Zarnetske et al., 2012; Chen et al., 2023). Thus, the source/sink terms R_i in Eq. (2) for the species DOC, DO, NO_3^- are given as:

$$R_{DO} = -V_O X \frac{C_{DOC}}{K_{DOC} + C_{DOC}} \frac{C_{DO}}{K_{DO} + C_{DO}} \quad (4)$$

$$R_{NO_3} = -V_N X \frac{K_I}{K_I + C_{DO}} \frac{C_{DOC}}{K_{DOC} + C_{DOC}} \frac{C_{NO_3}}{K_{NO_3} + C_{NO_3}} \quad (5)$$

$$R_{DOC} = R_{DO} + 1.25 R_{NO_3} + \rho_s \alpha_C (C_{POC} - K_d C_{DOC}) \quad (6)$$

where C_{DOC}, C_{DO}, C_{NO_3} and C_{POC} denote the concentration of DOC, DO, NO_3^-, and POC, respectively. V_O, V_N are the maximum microbial uptake rate of DO and NO_3^-, respectively. X

https://doi.org/10.5194/egusphere-2026-3760
Preprint. Discussion started: 7 July 2026

represents the microbial biomass per bulk volume of sediments. K_{DOC}, K_{DO}, K_{NO_3} are the half saturation constants of DOC, DO, NO_3^-, respectively. K_I is the inhibition constant. ρ_s denotes the bulk density of sediments. α_C represents the first-order mass transfer coefficient between POC and DOC. K_d denotes the distribution coefficient.

The microbial growth is simulated with the growth-death model expressed by (Caruso et al., 2017; Ping et al.,2020; Xian et al., 2019):

$$\frac{\partial X}{\partial t} = Y\left(1-\frac{X}{\rho_X \theta_0}\right)\left|R_{DO}+1.25R_{NO_3}\right| - k_d X \tag{7}$$

where Y is the yield coefficient, k_d denotes the endogenous decay coefficient, θ_0 is the initial porosity without microbial biomass, ρ_X represents the density of microbial biomass. The term $1-X/\rho_X\theta_0$ is introduced into Eq. (7) to account for the microbial self-limitation effect due to the limited pore spaces (Brovelli et al., 2009; Samsó et al., 2016).

With biomass growth, the porosity θ changes with time and is the function of θ_b:

$$\theta = \theta_0 - \theta_b \tag{8}$$

θ_b represents the microbial biomass volume per volume of sediments, and can be calculated by X/ρ_X. The sediment hydraulic conductivity K also varies in response to biofilm-induced changes in porosity. Here we adopted the biofilm-plug formation model (Vandevivere, 1995) to describe the relationship between K and θ:

$$\frac{K(\theta_r)}{K_0} = F(\theta_r)\theta_r^2 + \left[1-F(\theta_r)\right]\frac{K_{\min}/K_0}{\left[K_{\min}/K_0 + (1-\theta_r)(1-K_{\min}/K_0)\right]},$$
$$F(\theta_r) = \exp\left[-0.5\left(\frac{1-\theta_r}{1-\theta_{rc}}\right)^2\right] \tag{9}$$

https://doi.org/10.5194/egusphere-2026-3760
Preprint. Discussion started: 7 July 2026

where θ_r represents the relative porosity and equals to θ/θ_0, K_{min} is the minimum hydraulic conductivity corresponding to θ_r =0 at which pore spaces are completely occupied by biomass. θ_{rc} denotes a critical value of θ_r, and θ_r=θ_{rc} corresponds to the transition from the biofilm formations (phase I) to the plug formations (phase II) because of biofilm shearing in phase I then forming plug in phase II (Seifert and Engesgaard, 2012; Vandevivere, 1995).

2.2 Model Initial and Boundary Conditions, and Parameterisation and Scenario Simulations

The model simulations are setup for repeating ripple-induced HZs (Figure 1a). The water-sediment interface is assigned as a constant pressure boundary for porous media flow and an open boundary for solute transport in the porous media. The pressure profile along the water-sediment interface is derived through simulations of turbulent flow over the repeating ripples by numerically solving the Reynolds-averaged Navier-Stokes equations in steady state using the k-ω closure scheme (See Cardenas & Wilson (2007) for the further details of the model establishment and validation). The lateral sides for the solute transport are implemented as a spatially periodic boundary for both pressure and concentration, with a prescribed pressure drop $\triangle P$ that is consistent to the turbulence model. No flow and no flux are assigned to the bottom boundary. Two scenarios of stream nutrients, i.e., pristine (C_{s0}; DOC=5 mg/L, NO_3^-=2 mg/L) and polluted (C_{s0}; DOC=20 mg/L, NO_3^-=10 mg/L) and two stream flow velocity conditions (U=0.2 m/s, 0.8 m/s) are considered. The numerical model parameters governing porous media flow, solute reactive transport, microbial dynamics (growth and death), and biofilm-induced bioclogging were calibrated using experimental data from the laboratory-scale flume study conducted by Quick et al. (2016). The detailed validation procedures and outcomes presented in Section 3.1, and the model parameters are summarized in Table 1.

https://doi.org/10.5194/egusphere-2026-3760
Preprint. Discussion started: 7 July 2026

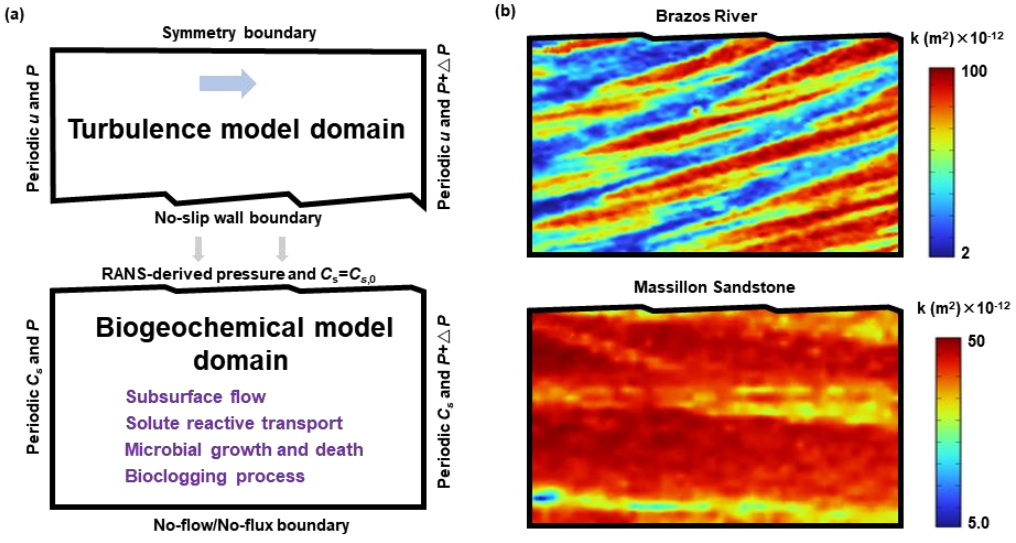

Figure 1. Modeling scheme. (a) The simulated processes, boundary condition configurations for the stream water turbulent flow (top part), and the solute reactive transport in streambeds (bottom part). (b) Two realistic permeability field adopted in the present study.

The datasets of spatial distribution of initial permeability and OM content are respectively created based on the images of the permeability field of the Massillon Sandstone and the climbing ripple deposits of the Brazos River from the Figures 1a and 1c of Sawyer & Cardenas (2009) (Figure 1b). The permeability field of the Massillon Sandstone indicates a slightly sloping (dips from 10° to 20°) and stratified heterogeneous sedimentary structure with a variance of 0.15. For the Brazos River, the image of climbing ripple deposits shows sloping bimodal deposits consisting of organic-scare sand and organic-rich silt with a variance of 1. We converted the color images into greyscale images. For the Massillon Sandstone, for the greyscale value of 1 and 0, the log-permeability values of -11.5 to -10.3 were respectively assigned, and the OM content of 0.5% and 0.1% were respectively given. These are typical values for sandy sediments (Sawyer, 2015). For the Brazos River, the log-permeability values of -10 to -12 and

https://doi.org/10.5194/egusphere-2026-3760
Preprint. Discussion started: 7 July 2026

the OM content of 0.2% and 2% are respectively given to the greyscale value of 1 and 0. Linear interpolation was applied to derive values between the upper and lower limits for the intermediate greyscale values. The two datasets represent low and moderate heterogeneity in permeability (K) and OM content, respectively (Bardini et al., 2013; Sawyer & Cardenas, 2009). While the variances in ln(K) and OM content are smaller compared to those reported in studies of large-scale heterogeneous fluvial systems (e.g., Genereaux et al., 2008; Kalbus et al., 2009), this study focuses on small-scale heterogeneity within fluvial bedforms associated with a single depositional facies, thereby isolating the effects of localized sediment variability.

The heterogeneous models with the microbial growth and the interactions between flow, nutrients and biofilm growth are called as *Hetero. Sed. & Bio. Growth* model. We also establish two sets of equivalent homogeneous model. In the first set, called as *Homo. Sed. & Bio. Growth* model, the equivalent permeability tensors of the heterogeneous sediments and the arithmetically weighted averages of OM content are used as the initial values. Microbial growth and the interactions between flow, nutrients and biofilms are included in the model. In the second set, called as *Hetero. Sed. & Const. Bio.* model, the datasets of heterogeneous permeability and OM distribution are adopted. Instead of simulating microbial growth processes, the arithmetically weighted average of the functional microbial biomass distribution of the *Hetero. Sed. & Bio. Growth*. model throughout the entire simulated period is applied. The importance of sedimentary heterogeneity (*Hetero. Sed. & Bio. Growth* vs. *Homo. Sed. & Bio. Growth*) and microbial heterogeneity (*Hetero. Sed. & Bio. Growth* vs. *Hetero. Sed. & Const. Bio.*) can be isolated by the comparisons of these experiments. In *Homo. Sed. & Bio. Growth* model, the equivalent permeability tensors for the Massillon Sandstone k_M and the Brazos River k_B were calculated following the method of Durlofsky (1991):

https://doi.org/10.5194/egusphere-2026-3760
Preprint. Discussion started: 7 July 2026

$$k_M = \begin{bmatrix} 8.36 & -0.0011 \\ -0.0011 & 8.25 \end{bmatrix} \times 10^{-11} \quad \mathrm{m}^2 \tag{221}$$

$$k_B = \begin{bmatrix} 4.87 & 0.44 \\ 0.44 & 4.40 \end{bmatrix} \times 10^{-11} \quad \mathrm{m}^2 \tag{222}$$

Eqs. (1-14) are numerically solved by the finite-element software COMSOL Multiphysics. For this, 2-D model domains are discretized using triangular elements. The triangular element size is 0.5 mm at the water-sediment interface and generally increase to 3.5 mm towards the bottom boundary with a factor of 1.05. To determine the initial values for model parameterisation, the *Hetero. Sed. & Bio. Growth*. models are first run for a period of 180 d to reach a quasi-steady state under low stream nutrient concentrations of DOC=2 mg/L, NO_3^-=1 mg/L, DO=8 mg/L. The model simulations are run for a period of 730 d, which is sufficiently long for microbial communities to fully acclimate from the initial condition to a new hydro-biogeochemical environment. All simulated model scenarios are summarized in Table 2.

Table 1. Summary of numerical model parameters.

Parameters	2-D flume model	Model simulations	Source
Physical parameters			
Initial porosity (θ_0, -)	0.38	0.38	1
Initial permeability (k_0, m/s)	5.5×10^{-4}	1×10^{-10}-1×10^{-2}	2
		$1\times10^{-11.5}$-$1\times10^{-10.3}$	
Reactive transport parameters		1×10^{-9}	
Molecular diffusion coefficient of (D_m, m^2/s)	1×10^{-9}	1×10^{-9}	C
Longitudinal dispersivity (α_L, m)	1.0×10^{-2}	1.0×10^{-3}	2
Transverse dispersivity (α_L, m)	1.0×10^{-3}	1.0×10^{-4}	2

https://doi.org/10.5194/egusphere-2026-3760
Preprint. Discussion started: 7 July 2026

Maximum specific uptake rate for O_2 (V_O, 1/h)	0.32	0.32	C
Half-saturation constants for DOC (K_{DOC}, mg/L)	18	18	C
Half-saturation constant for DO (K_{DO}, mg/L)	5.0	5.0	C
Maximum specific uptake rate for NO_3^- (V_N, 1/h)	0.28	0.28	C
Half-saturation constant for NO_3^- (K_{NO3}, mg/L)	1.0	1.0	C
Inhibition constant (K_I, mg/L)	0.8	0.8	C
Mass transfer coefficient for DOC (α_C; 1/hr)	5×10^{-4}	5×10^{-5}	3
Distribution coefficient of DOC (K_d; L/kg)	10	7500	3
Bulk density (ρ_s; kg/m^3)	1600	1600[c]	C
Initial organic matter content (POC_0)	0.15%	0.2%-2% 0.1%-0.5%	3
Biofilm growth parameters			
Yield coefficient (Y, -)	0.15	0.15	C
Decay rate coefficient (k_d, d^{-1})	0.1	0.1	C
Density of biomass (ρ_X, kg/m^3)	1.5	1.5	C
Biofilm-plug formation model			

https://doi.org/10.5194/egusphere-2026-3760
Preprint. Discussion started: 7 July 2026

Minimum relative hydraulic conductivity (K_{min}/ K_0, -)	1×10^{-4}	1×10^{-4}	C
Critical relative porosity (θ_{rc}, -)	0.75	0.75	C

Source: 1. Quick et al., 2016; 2. Sawyer & Cardenas, 2009; Bardini et al., 2013; 3. Zarnetske et al., 2012; Pescimoro et al.,2019; C. The parameter values are calibrated from the experimental data of Quick et al. et al. (2016).

Table 2. Summary of the numerical experiments carried out in this study.

Experiment	Sediment and functional microbial biomass	Parameters
Hetero. Sed. & Bio. Growth model	Heterogeneous sediments, with biomass growth	See Table S1
Homo. Sed. & Bio. Growth model	Equivalent homogeneous sediments, with biomass growth	Based on initial values of *Hetero. Sed. & Bio. Growth* models, Equivalent permeability tensors and arithmetically weighted averages of OM content are used as initial values.
Hetero. Sed. & Const. Bio. model	Heterogeneous sediments, constant biomass	*K* is constant and set as initial values of *Hetero. Sed. & Bio. Growth* model. *X* is constant and uniform and calculated as arithmetically weighted average of microbial biomass across entire space and time in *Hetero. Sed. & Bio. Growth* models.

https://doi.org/10.5194/egusphere-2026-3760
Preprint. Discussion started: 7 July 2026

3 Results and Discussions

3.1 Model Validation

To ensure the 2D numerical model's reliability, we simulate the nitrate reactive transport process in the hyporheic zones of the flume experiments by Quick et al. (2016) and compare with the experimental data. The flume experiment, conducted in 2015, employed artificially constructed dune morphologies with a wavelength of 0.7 m and amplitude of 0.09 m. The sediment bed was composed of 90% quarried sand and 10% microbial-inoculated sand, and the sediment contains 0.15% particulate organic matter (Black cottonwood (i.e., Populus trichocarpa) leaves). Over a 13-week experimental duration, nitrate loading was controlled by injecting KNO_3 to achieve a surface water concentration of 10 mg L^{-1} by day 62. Spatial and temporal monitoring included continuous DO measurements using in situ sensors, and discrete sampling of porewater chemistry. See Quick et al. (2016) for the details of the flume experiment. Model calibration focused on optimizing the parameters of porous flow, biogeochemical reaction and biofilm growth kinetics by fitting the simulation results to observed data. As portrayed in Figure 2, the simulated results generally agree well with the experimental data of solute residence time (RT) distributions, and the distributions of DO and NO_3^- concentrations. This validation indicates the numerical model can effectively capture the coupled hydrodynamic-biogeochemical dynamics in HZ systems. The calibrated numerical model parameters are listed in Table 1.

https://doi.org/10.5194/egusphere-2026-3760
Preprint. Discussion started: 7 July 2026

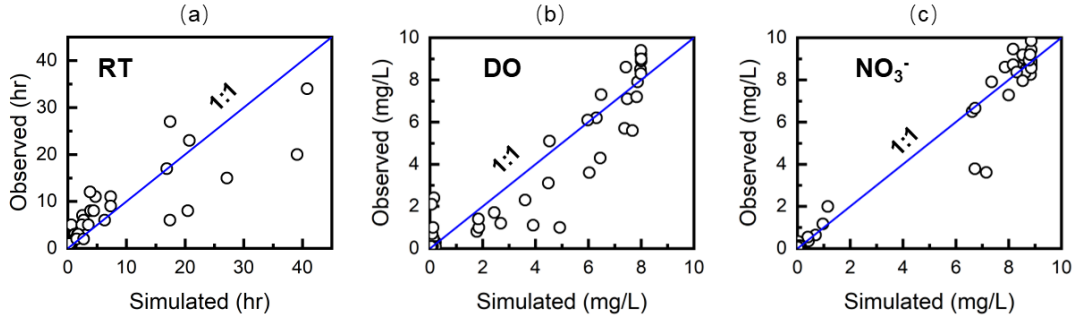

Figure 2. Comparisons between simulated and observed by Quick et al. et al. (2016) of (a) residence time (RT) distribution, (b) DO, and (c) NO_3^-.

3.2 Effect of Sedimentary heterogeneity and microbial heterogeneity on Nitrate Removal in HZs

The outcomes of the different senario simulations indicate that, compared to their respective homogeneous analogues, the spatial variability in functional microbial biomass presents a decisive role on enhanced removal of nitrate in the hyporheic zones. In contrast, small-scale heterogeneity of physical streambed properties (i.e., permeability) and chemical (i.e., OM content) heterogeneities turned out to have negligible effect.

Figure 3 illustrates that in the *Hetero. Sed. & Bio. Growth* models parameterized to represent Brazos River conditions, five hyporheic flow cells driven by ripples develop within streambed sediments. Under nutrient enrichment from fluvial inputs, microbial biomass proliferates near the water-sediment interface, eventually forming a bioactive layer at the streambed surface (Figure 3a). Concurrently, biofilm-induced clogging generates a progressive reduction of permeability in a layer aligned with this active zone (Figure 3b). In response to such reduced permeability and intensified microbial nutrient consumption, transport fronts of DOC, DO, and NO_3^-, alongside DOC and nitrate reduction hotspots, migrated further toward the

https://doi.org/10.5194/egusphere-2026-3760
Preprint. Discussion started: 7 July 2026

sediment-water interface (Figure 3c-3g).

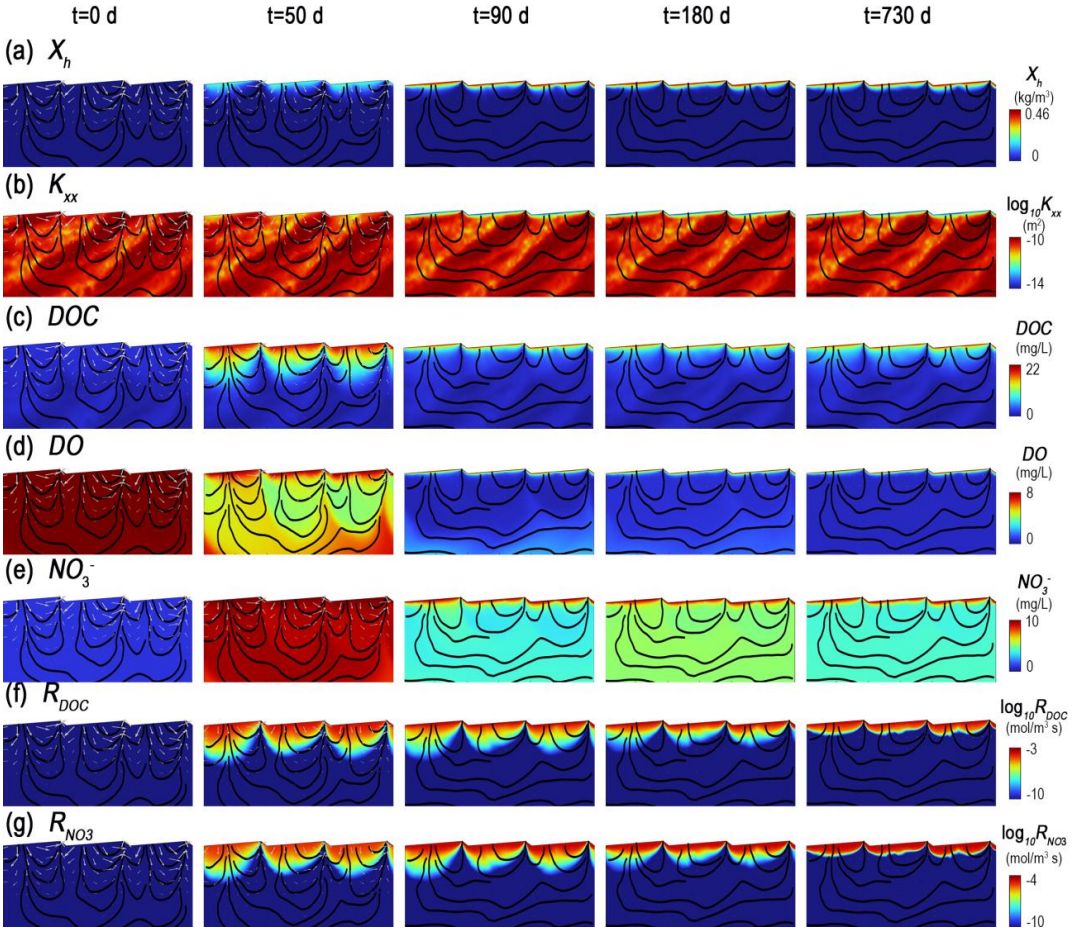

Figure 3. Evolution of spatial distribution of (a) X_h, (b) K_{xx}, (c) DOC, (d) DO, (e) NO_3^-, (f) R_{DOC}, (g) R_{NO3} over time in the *Hetero. Sed. & Bio. Growth* model of the Brazos River under average stream flow velocity U=0.8 m/s.

https://doi.org/10.5194/egusphere-2026-3760
Preprint. Discussion started: 7 July 2026

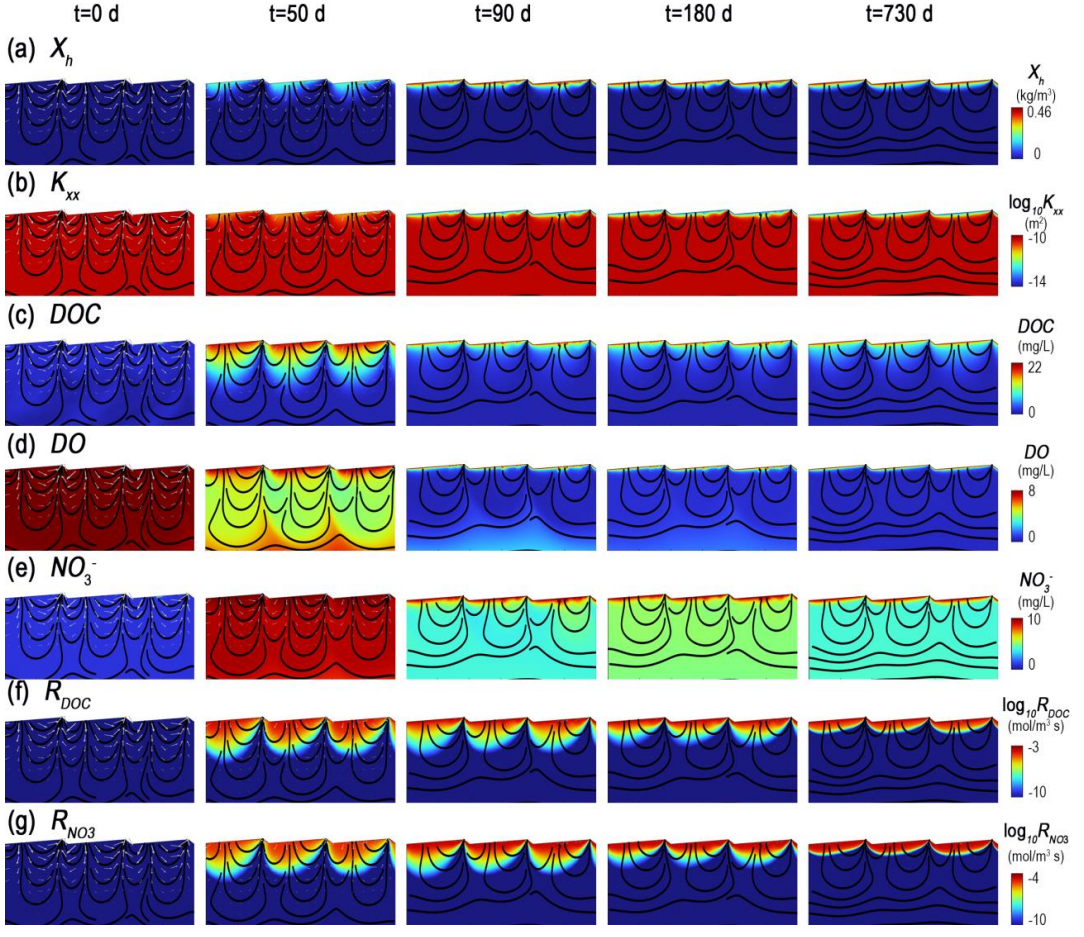

Figure 4. Evolution of spatial distribution of (a) X_h, (b) K_{xx}, (c) DOC, (d) DO, (e) NO_3^-, (f) R_{DOC}, (g) R_{NO3} over time in the *Homo. Sed. & Bio. Growth* model of the Brazos River under average stream flow velocity U=0.8 m/s.

Figure 4 shows the evolutions of the spatial distribution of X_h, K_{xx}, DOC, DO, NO_3^-, R_{DOC} and R_{NO_3} for the *Homo. Sed. & Bio. Growth* model which considered an equivalent permeability and POC content and included microbial growth. By comparing Figure 3 and Figure 4, only slight differences occur between the results of *Hetero. Sed. & Bio. Growth* and *Homo. Sed. & Bio. Growth* models. Specifically, the plume fronts are slightly jagged in the *Hetero. Sed. & Bio.*

https://doi.org/10.5194/egusphere-2026-3760
Preprint. Discussion started: 7 July 2026

Growth model due to the heterogeneous permeability and POC content, while they are relatively smooth in the results of the *Homo. Sed. & Bio. Growth* model because of more homogeneous distribution of permeability and POC content. To quantify the effect of sedimentary heterogeneity on nitrate removal, we compare the total nitrate removal R_N by integrating removal rate of nitrate across the 2-D model domain over the simulated period. As indicated in Table 3, the differences of R_N between *Hetero. Sed. & Bio. Growth* and *Homo. Sed. & Bio. Growth* model over various scenarios range from 2.3%-10.1% for the Brazos River, and 0.6%-7.6% for the Massillon Sandstone. This only minor effect of sedimentary heterogeneity on nitrate removal can be attributed to the followings: With biofilm growth, the permeability of the sediment near the water-sediment interface is gradually reduced (Figure 3b and Figure 4b). In response, the HZ size diminishes, and therefore the effect of sediment heterogeneity in the deeper sediments on nitrate removal is weakened. In consequence, the small-scale sedimentary heterogeneity including spatial variabilities in permeability and OM content only have slight effect on the removal of nitrate in HZs.

Table 3. Total nitrate removal (R_N) of different model simulation scenarios

Stream conditions (U [m/s], C [mg/L], NO_3^{-1} [mg/L])		R_N (g/m)			Errors (%)	
		Hetero. Sed. & Bio. Growth	*Homo. Sed. & Bio. Growth*	*Hetero. Sed. & Const. Bio.*	*Homo. Sed. & Bio. Growth*	*Hetero. Sed. & Const. Bio.*
Brazos River	U=0.2, C_0= 5, NO_3^-=2	3.7	3.3	0.8	10.1	79.5
	U=0.2, C_0= 20, NO_3^{-1}=10	67.8	64.7	6.1	4.6	91.0

https://doi.org/10.5194/egusphere-2026-3760
Preprint. Discussion started: 7 July 2026

	U=0.8, C_0= 5, NO_3^-=2	13.9	13.4	3.7	3.4	73.0
	U=0.8, C_0= 20, NO_3^-=10	176.4	180.4	21.0	2.3	88.1
Massillon Sandstone	U=0.2, C_0= 5, NO_3^-=2	2.7	2.7	0.2	0.6	91.1
	U=0.2, C_0= 20, NO_3^-=10	91.3	84.3	2.2	7.6	97.6
	U=0.8, C_0= 5, NO_3^-=2	20.5	20.6	3.5	0.7	82.8
	U=0.8, C_0= 20, NO_3^-=10	320.2	344.3	22.6	7.5	92.9

Note. Errors=|$R_{N\text{-}Baseline}$ - $R_{N\text{-}Set\ 1}$ (or $R_{N\text{-}Set\ 2}$) |/ $R_{N\text{-}Baseline}$×100%, where the *Baseline* denotes the *Hetero. Sed. & Bio. Growth* model, the *set 1* represents the *Homo. Sed. & Bio. Growth model,* and the *set 2* denotes the *Hetero. Sed. & Const. Bio.* model.

In contrast, significant differences exist in the spatiotemporal distributions of DOC, DO and NO_3^-, and R_{DOC}, R_{NO_3} between the *Hetero. Sed. & Bio. Growth* and *Hetero. Sed. & Const. Bio.* models, which account for the sedimentary heterogeneity while assuming constant and uniform functional microbial biomass distributions. As described in Figures 3 and 5, the penetration depths of DOC, DO and NO_3^- are greater in the *Hetero. Sed. & Const. Bio.* models than the *Hetero. Sed. & Bio. Growth* models after t=50 d. This is because the microbial biomass concentration is assumed uniform and constant, and is much lower in the hyporheic zone for the *Hetero. Sed. & Const. Bio.* models than that in the superficial layer of *Hetero. Sed. & Bio. Growth* models, and thus the biofilm-induced bioclogging effect is much weaker. Accordingly, the hotspots of aerobic respiration are more pronounced and the hotspots of denitrification occur

https://doi.org/10.5194/egusphere-2026-3760
Preprint. Discussion started: 7 July 2026

deeper in the *Hetero. Sed. & Const. Bio.* models. In comparisons, in the *Hetero. Sed. & Bio. Growth* models, the aerobic respiration mainly in the superficial bioactive layer, while the denitrification occurs in the shallower sediments. These discrepancies are also quantitively evaluated using R_N in Table 3. The differences of R_N between the *Hetero. Sed. & Bio. Growth* and *Hetero. Sed. & Const. Bio.* models in the various scenarios range from 73.0% to 91.0% for the Brazos River, and 82.6 to 97.6% for the Massillon Sandstone. The R_N ratio of the *Hetero. Sed. & Bio. Growth* and *Hetero. Sed. & Const. Bio.* models can reach as much as 41.3. Thus, functional microbial biomass heterogeneity has a substantial impact on the enhanced removal of nitrate in contrast to the hyporheic zone models assuming constant and uniform microbial biomass. See Figures S2-S7 for the comparisons of the Brazos River under different stream flow velocity and nutrient conditions.

Some pioneering works on this issue include, for example, Bardini et al. (2013) who indicated that the sole permeability heterogeneity has negligible effects on nitrogen cycling in HZs. Further, Sawyer (2015) presented that the combined effects of permeability and OM content heterogeneity can largely enhance the upwelling groundwater-borne nitrate removal. The enhanced nitrate removal is attributed to the mixing effects of waters with different chemical components at the oxic-anoxic interfaces and create the localized anoxic microzones in fine structures of heterogeneous sediments that can effectively promote denitrification. As such, it is expected that sedimentary heterogeneity would enhance the nitrate removal of HZs in contrast to the equivalent homogeneous sediments. However, unexpectedly, the present study shows that the sedimentary heterogeneity has only small impact on nitrate removal, despite under the existence of spatial variability in permeability and OM content. Thus, it is unnecessary to take tremendous

https://doi.org/10.5194/egusphere-2026-3760
Preprint. Discussion started: 7 July 2026

336 labor for acquiring the small-scale sedimentary heterogeneity to improve prediction accuracy of
337 HZs' nitrate removal models.

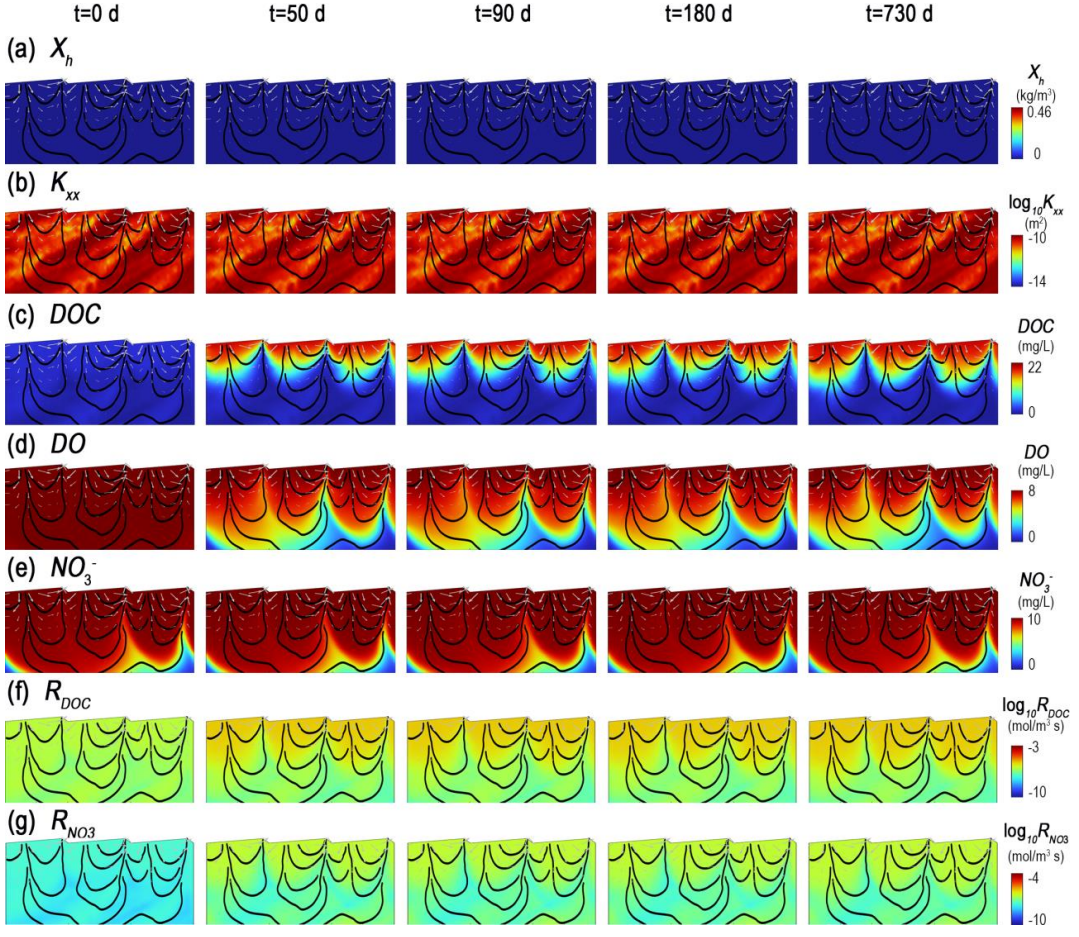

338

339 Figure 5. Evolution of spatial distribution of (a) X_h, (b) K_{xx}, (c) DOC, (d) DO, (e) NO_3^-, (f) R_{DOC},
340 (g) R_{NO3} over time in the *Hetero. Sed. & Const. Bio.* model of the Brazos River under average
341 stream flow velocity U=0.8 m/s.

342 Compared to the negligible effect to sedimentary heterogeneity, the present study shows
343 that spatial heterogeneity in functional microbial biomass momentously enhances the nitrate
344 removal of HZs in relative to the streambed assuming uniform microbial distribution. Under the

https://doi.org/10.5194/egusphere-2026-3760
Preprint. Discussion started: 7 July 2026

stream-borne nutrient stimulations, microbial biomass grows mostly near the water-sediment interface, while it is relatively sparse in the deep sediments. The hotspots of denitrification develop adjacent to the superficial bioactive layer under the regulation of nutrients, DO and microbial distributions. The aggregation of functional microbial biomass near the water-sediment interface importantly increases the denitrification rate across the hotspot as well as the nitrate removal capacity of streambed sediments, in contrast to the HZs in the streambed using the common assumption of constant and uniform microbial biomass. By conducting flume experiments, De Falco et al. (2018) compared the microbial consumption rate of DO in disturbed (homogeneous biomass distribution) and stationary (concentrated biomass near water-sediment interface) bed forms. The enhanced effect of the concentrated functional microbial biomass is documented by the elevated DO consumption rate in the stationary bed forms under various stream flow velocity. Consequentially, microbial heterogeneity plays a more decisive role on regulation of nitrate removal of HZs than sedimentary heterogeneity. In field settings, it is critical to get the spatiotemporal distribution of functional microbial biomass in HZs, especially near the water-sediment interface, otherwise significant errors of nitrate removal would be induced by the typical assumption of constant and uniform microbial biomass.

5 Conclusions

Under the feedbacks of porous flow, reactive transport of nutrients and microbial growth, sedimentary heterogeneity including physical (e.g., permeability), chemical (e.g., OM content) and microbial heterogeneity coexist and interconnect in HZs of streambeds. This study is the first to reveal the regulations of sedimentary and microbial heterogeneities on nitrate removal of HZs. For small-scale heterogeneous riverbeds, the influence of sedimentary heterogeneity on nitrate removal of HZs can be negligible, while the impact of the heterogeneous distribution of

https://doi.org/10.5194/egusphere-2026-3760
Preprint. Discussion started: 7 July 2026

functional microorganisms is crucial. These novel discoveries have important implications for the conceptualization and parameterization of heterogeneous riverbed models. These include the possibility of using equivalent homogeneous riverbed models as substitutes for actual heterogeneous riverbeds, thereby overcoming the significant challenges associated with obtaining sediment heterogeneity information. In contrast, accurate acquisition of information regarding the heterogeneous distribution of functional microorganisms in HZs is crucial for improving model estimation accuracy.

Supporting information

Additional details of the model simulation results were displayed in the supporting information.

Data availability

All raw data can be provided by the first author upon request.

Competing interest

The authors declare that they have no conflict of interest.

Author contribution

Conceptualization: YX, ZW

Formal analysis: YX

Funding acquisition: YX, ZW

Investigation: YX, ZW

Methodology: YX

Writing-original draft: YX

Writing-review and editing: ZW, SK

Project administration: ZW

https://doi.org/10.5194/egusphere-2026-3760
Preprint. Discussion started: 7 July 2026

Acknowledgments

This study was financially supported by the National Natural Science Foundation of China (No. 42572305, U23A2042). The project was supported by the "CUG Scholar" Scientific Research Funds at China University of Geosciences (Wuhan) (Project No.2023067).

References

Bardini, L., Boano, F., Cardenas, M. B., Sawyer, A. H., Revelli, R., and Ridolfi, L.: Small-scale permeability heterogeneity has negligible effects on nutrient cycling in streambeds, Geophys. Res. Lett. 40(6), 1118-1122, https://doi.org/10.1002/grl.50224, 2013.

Barnes, R. T., Sawyer, A. H., Tight, D. M., Wallace, C. D., and Hastings, M. G.: Hydrogeologic controls of surface water-groundwater nitrogen dynamics within a tidal freshwater zone, J. Geophys. Res.: Biogeosci. 124(11), 3343-3355, https://doi.org/10.1029/2019JG005164, 2019.

Boano, F., Harvey, J. W., Marion, A., Packman, A. I., Revelli, R., Ridolfi, L., and Wörman, A.: Hyporheic flow and transport processes: Mechanisms, models, and biogeochemical implications, Rev. Geophys. 52(4), 603-679, https://doi.org/10.1002/2012RG000417, 2014.

Briggs, M. A., Day-Lewis, F. D., Zarnetske, J. P., and Harvey, J. W.: A physical explanation for the development of redox microzones in hyporheic flow, Geophys. Res. Lett. 42(11), 4402-4410, https://doi.org/10.1002/2015GL064200, 2015.

Brovelli, A., Malaguerra, F., and Barry, D. A.: Bioclogging in porous media: Model development and sensitivity to initial conditions, Environ. Model. Softw. 24(5), 611-626, https://doi.org/10.1016/j.envsoft.2008.10.001, 2009.

https://doi.org/10.5194/egusphere-2026-3760
Preprint. Discussion started: 7 July 2026

Cardenas, M. B., and Wilson, J. L.: Dunes, turbulent eddies, and interfacial exchange with permeable sediments, Water Resour. Res. 43(8), W08412, https://doi.org/10.1029/2006WR005787, 2007.

Cardenas, M. B., Wilson, J. L. and Zlotnik, V. A.: Impact of heterogeneity, bed forms, and stream curvature on subchannel hyporheic exchange, Water Resour. Res. 40, W08307. https://doi.org/10.1029/2004WR003008, 2004.

Caruso, A., Boano, F., Ridolfi, L., Chopp, D. L., and Packman, A.: Biofilm-induced bioclogging produces sharp interfaces in hyporheic flow, redox conditions, and microbial community structure, Geophys. Res. Lett. 44, 4917-4925. https://doi.org/10.1002/2017GL073651, 2017.

Chen, K., Guo, Z., Zhan, Y., Roden, E. E., and Zheng, C.: Heterogeneity in permeability and particulate organic carbon content controls the redox condition of riverbed sediments at different timescales, Geophys. Res. Lett. 51(11), e2023GL107761. https://doi.org/10.1029/2023GL107761, 2024.

Chen, K., Roden, E. E., and Zheng, C.: Hydrological Controls on Riverbed Methane Emissions: A Numerical Investigation of Hydrodynamic and Ebullitive Mechanisms from Site to Basin Scales, Environ. Sci. Technol. 59(29), 15170-15180, https://doi.org/10.1021/acs.est.5c03453, 2025.

Chen, K., Yang, S., Roden, E. E., Chen, X., Chang, K. Y., Guo, Z., ... and Zheng, C.: Influence of vertical hydrologic exchange flow, channel flow, and biogeochemical kinetics on CH4 emissions from rivers, Water Resour. Res. 59(12), e2023WR035341, https://doi.org/10.1029/2023WR035341, 2023.

https://doi.org/10.5194/egusphere-2026-3760
Preprint. Discussion started: 7 July 2026

435 Chowdhury, R. S., Zarnetske, J. P., Phanikumar, M. S., Briggs, M. A., Day-Lewis, F. D., and
436 Singha, K.: Formation criteria for hyporheic anoxic microzones: Assessing interactions of
437 hydraulics, nutrients, and biofilms, Water Resour. Res. 56(3), e2019WR025971,
438 https://doi.org/10.1029/2019WR025971, 2020.
439 Claret, C., Marmonier, P., Boissier, J. M., Fontvieille, D., and Blanc, P.: Nutrient transfer
440 between parafluvial interstitial water and river water: influence of gravel bar
441 heterogeneity, Freshw. Biol. 37(3), 657-670, https://doi.org/10.1046/j.1365-
442 2427.1997.00193.x, 1997.
443 De Falco, N., Boano, F., Bogler, A., Bar-Zeev, E., and Arnon, S.: Influence of stream-subsurface
444 exchange flux and bacterial biofilms on oxygen consumption under nutrient-rich
445 conditions, J. Geophys. Res.: Biogeosci. 123(7), 2021-2034,
446 https://doi.org/10.1029/2017JG004372, 2018.
447 Durlofsky, L. J.: Numerical calculation of equivalent grid block permeability tensors for
448 heterogeneous porous media, Water Resour. Res. 27(5), 699-708,
449 https://doi.org/10.1029/91WR00107, 1991.
450 Genereux, D. P., Leahy, S., Mitasova, H., Kennedy, C. D., and Corbett, D. R.: Spatial and
451 temporal variability of streambed hydraulic conductivity in West Bear Creek, North
452 Carolina, USA, J. Hydrol. 358(3-4), 332-353,
453 https://doi.org/10.1016/j.jhydrol.2008.06.017, 2008.
454 Gomez-Velez, J. D., Harvey, J. W., Cardenas, M. B., and Kiel, B.: Denitrification in the
455 Mississippi River network controlled by flow through river bedforms, Nat. Geosci. 8(12),
456 941-945, https://doi.org/10.1038/ngeo2567, 2015.

https://doi.org/10.5194/egusphere-2026-3760
Preprint. Discussion started: 7 July 2026

457 Gomez-Velez, J. D., Krause, S., and Wilson, J. L.: Effect of low-permeability layers on spatial
458 patterns of hyporheic exchange and groundwater upwelling, Water Resour. Res. 50(6),
459 5196-5215, https://doi.org/10.1002/2013WR015054, 2014.
460 Grant, S. B., Azizian, M., Cook, P., Boano, F., and Rippy, M. A.: Factoring stream turbulence
461 into global assessments of nitrogen pollution, Science, 359(6381), 1266-1269,
462 https://doi.org/10.1126/science.aap8074, 2018.
463 Gruber, N., and Galloway, J. N.: An Earth-system perspective of the global nitrogen cycle.
464 Nature, 451(7176), 293-296, https://doi.org/10.1038/nature06592, 2008.
465 Gu, C. H., Hornberger, G. M., Mills, A. L., Herman, J. S., and Flewelling, S. A.: Nitrate
466 reduction in streambed sediments: Effects of flow and bio-geochemical kinetics, Water
467 Resour. Res. 43, W12413, https://doi.org/10.1029/2007WR006027, 2007.
468 Harvey, J., and Gooseff, M.: River corridor science: Hydrologic exchange and ecological
469 consequences from bedforms to basins, Water Resour. Res. 51(9), 6893-6922.
470 https://doi.org/10.1002/2015WR017617, 2015.
471 Kalbus, E., Schmidt, C., Molson, J. W., Reinstorf, F., and Schirmer, M.: Influence of aquifer and
472 streambed heterogeneity on the distribution of groundwater discharge, Hydrol. Earth Syst.
473 Sci. 13(1), 69-77, https://doi.org/10.5194/hess-13-69-2009, 2009.
474 Knights, D., Sawyer, A. H., Barnes, R. T., Musial, C. T., and Bray, S.: Tidal controls on riverbed
475 denitrification along a tidal freshwater zone, Water Resour. Res. 53(1), 799-816.
476 https://doi.org/10.1002/2016WR019405, 2017.
477 Krause, S., Abbott, B. W., Baranov, V., Bernal, S., Blaen, P., Datry, T., ... and Zarnetzke, J. P.:
478 Organizational principles of hyporheic exchange flow and biogeochemical cycling in river

https://doi.org/10.5194/egusphere-2026-3760
Preprint. Discussion started: 7 July 2026

networks across scales, Water Resour. Res. 58(3), e2021WR029771, https://doi.org/10.1029/2021WR029771, 2022.

Krause, S., Lewandowski, J., Grimm, N. B., Hannah, D. M., Pinay, G., McDonald, K., et al.: Ecohydrological interfaces as hot spots of ecosystem processes: Ecohydrological interfaces as hot spots, Water Resour. Res. 53, 6359–6376, https://doi.org/10.1002/2016WR019516, 2017.

Krause, S., Tecklenburg, C., Munz, M., and Naden, E.: Streambed nitrogen cycling beyond the hyporheic zone: Flow controls on horizontal patterns and depth distribution of nitrate and dissolved oxygen in the upwelling groundwater of a lowland river, J. Geophys. Res.: Biogeosci. 118(1), 54-67, https://doi.org/10.1029/2012JG002122, 2013.

Martínez-Espinosa, C., Sauvage, S., Al Bitar, A., Green, P. A., Vörösmarty, C. J., and Sánchez-Pérez, J. M.: Denitrification in wetlands: A review towards a quantification at global scale, Sci. Total Environ. 754, 142398, https://doi.org/10.1016/j.scitotenv.2020.142398, 2021.

Molz, F. J., Widdowson, M. A., and Benefield, L. D.: Simulation of microbial growth dynamics coupled to nutrient and oxygen transport in porous media, Water Resour. Res. 22(8), 1207-1216, https://doi.org/10.1029/WR022i008p01207, 1986.

Pescimoro, E., Boano, F., Sawyer, A. H., and Soltanian, M. R.: Modeling influence of sediment heterogeneity on nutrient cycling in streambeds, Water Resour. Res. 55(5), 4082-4095, https://doi.org/10.1029/2018WR024221, 2019.

Ping, X., Jin, M., and Xian, Y.: Effect of bioclogging on the nitrate source and sink function of a hyporheic zone, J. Hydrol. 125425, https://doi.org/10.1016/j.jhydrol.2020.125425, 2020.

https://doi.org/10.5194/egusphere-2026-3760
Preprint. Discussion started: 7 July 2026

Ping, X., Xian, Y., and Jin, M.: Influence of bedform migration on nitrate reduction in hyporheic zones of heterogeneous sediments, Water Resour. Res. 58(11), e2022WR033258, https://doi.org/10.1029/2022WR033258, 2022.

Samsó, R., García, J., Molle, P., and Forquet, N.: Modelling bioclogging in variably saturated porous media and the interactions between surface/subsurface flows: Application to constructed wetlands, J. Environ. Manag. 165, 271-279, https://doi.org/10.1016/j.jenvman.2015.09.045, 2016.

Sawyer, A. H.: Enhanced removal of groundwater-borne nitrate in heterogeneous aquatic sediments, Geophys. Res. Lett. 42(2), 403-410, https://doi.org/10.1002/2014GL062234, 2015.

Sawyer, A. H., and Cardenas, M. B.: Hyporheic flow and residence time distributions in heterogeneous cross-bedded sediment, Water Resour. Res. 45(8), W08406, https://doi.org/10.1029/2008WR007632, 2009.

Seifert, D., and Engesgaard, P.: Sand box experiments with bioclogging of porous media: Hydraulic conductivity reductions, J. Contam. Hydrol. 136, 1-9, https://doi.org/10.1016/j.jconhyd.2012.04.007, 2012.

Stegen, J. C., Johnson, T., Fredrickson, J. K., Wilkins, M. J., Konopka, A. E., Nelson, W. C., ... and Zachara, J.: Influences of organic carbon speciation on hyporheic corridor biogeochemistry and microbial ecology, Nat. Commun. 9(1), 585, https://doi.org/10.1038/s41467-018-02922-9, 2018.

Vandevivere, P.: Bacterial clogging of porous media: a new modelling approach. Biofouling, 8(4), 281-291, https://doi.org/10.1080/08927019509378281, 1995.

https://doi.org/10.5194/egusphere-2026-3760
Preprint. Discussion started: 7 July 2026

Wallace, C. D., Sawyer, A. H., Soltanian, M. R., and Barnes, R. T.: Nitrate removal within heterogeneous riparian aquifers under tidal influence, Geophys. Res. Lett. 47(10), e2019GL085699. https://doi.org/10.1029/2019GL085699, 2020.

Wallace, C. D., Tonina, D., McGarr, J. T., de Barros, F. P., and Soltanian, M. R.: Spatiotemporal dynamics of nitrous oxide emission hotspots in heterogeneous riparian sediments, Water Resour. Res. 57(12), e2021WR030496, https://doi.org/10.1029/2021WR030496, 2021.

Xian, Y., Jin, M., Zhan, H., and Liang, X.: Permeable biofilms can support persistent hyporheic anoxic microzones, Geophys. Res. Lett. 49(14), e2021GL096948, https://doi.org/10.1029/2021GL096948, 2022.

Xian, Y., Jin, M., Zhan, H., and Liu, Y.: Reactive transport of nutrients and bioclogging during dynamic disconnection process of stream and groundwater, Water Resour. Res. 55(5), 3882-3903, https://doi.org/10.1029/2019WR024826, 2019.

Xian, Y., Wen, Z., Jin, M., Liang, X., and Jakada, H.: Groundwater-borne nitrate removal within heterogeneous sediments under interactions between hydraulics, nutrients, and biofilms, J. Hydrol. 616, 128777, https://doi.org/10.1016/j.jhydrol.2022.128777, 2023.

Zarnetske, J. P., Haggerty, R., Wondzell, S. M., and Baker, M. A.: Labile dissolved organic carbon supply limits hyporheic denitrification, J. Geophys. Res.: Biogeosci. 116, G04036, https://doi.org/10.1029/2011JG001730, 2011.

Zarnetske, J. P., Haggerty, R., Wondzell, S. M., Bokil, V. A., and González-Pinzón, R.: Coupled transport and reaction kinetics control the nitrate source-sink function of hyporheic zones, Water Resour. Res. 48, W11508, https://doi.org/10.1029/2012WR011894, 2012.

https://doi.org/10.5194/egusphere-2026-3760
Preprint. Discussion started: 7 July 2026

543 Zhang, Z., Xian, Y., Ping, X., Jin, M., and Guo, H.: Effect of microbial growth and electron
544 competition on nitrous oxide source and sink function of hyporheic zones, J. Hydrol. 638,
545 131585, https://doi.org/10.1016/j.jhydrol.2024.131585, 2024.
546 Zhang, Z., Xian, Y., Ping, X., Zhou, R., Guo, H., and Xue, P.: Controls of streambed sediment
547 heterogeneity and dynamic microbial biomass growth on nitrous oxide dynamics in
548 hyporheic zones, J. Hydrol. 135484, https://doi.org/10.1016/j.jhydrol.2026.135484, 2026.